A&A 635, A201 (2020)
https://doi.org/10.1051/0004-6361/201936840


Astronomy & Astrophysics

# Asymmetrical nebula of the M 33 variable GR 290 (WR/LBV)⋆

Olga V. Maryeva[1,2], Gloria Koenigsberger[3], Sergey V. Karpov[4,5,6], Tatiana A. Lozinskaya[2], Oleg V. Egorov[2], Corinne Rossi[7,8], Massimo Calabresi[9], and Roberto F. Viotti[10]

[1] Astronomical Institute of the Czech Academy of Sciences, Fričova 298, 25165 Ondřejov, Czech Republic
e-mail: olga.maryeva@asu.cas.cz
[2] Lomonosov Moscow State University, Sternberg Astronomical Institute, Universitetsky pr. 13, 119234 Moscow, Russia
[3] Instituto de Ciencias Físicas, Universidad Nacional Autónoma de México, Ave. Universidad s/n, 62210 Cuernavaca, Morelos, México
[4] Institute of Physics of the Czech Academy of Sciences, 18221 Prague, Czech Republic
[5] Special Astrophysical Observatory of the Russian Academy of Sciences, 36916 Nizhnij Arkhyz, Russia
[6] Laboratory "Fast Variable Processes in the Universe", Kazan Federal University, 420008 Kazan, Russia
[7] Physics Department, Università di Roma "La Sapienza", Piazza le Aldo Moro 5, 00185 Roma, Italy
[8] INAF, Osservatorio Astronomico di Roma, Via Frascati 33, 00077 Monte Porzio Catone, Italy
[9] Associazione Romana Astrofili, Via Carlo Emanuele I, n°12A, 00185 Roma, Italy
[10] INAF – Istituto di Astrofisica e Planetologia Spaziali di Roma (IAPS-INAF), Via del Fosso del Cavaliere 100, 00133 Roma, Italy

Received 3 October 2019 / Accepted 22 February 2020

**ABSTRACT**

*Context.* GR 290 (M 33 V0532 = Romano's star) is a luminous M 33 object undergoing photometric variability typical for luminous blue variable stars. It lies inside the Wolf-Rayet region in the Hertzsprung-Russell diagram and possesses a WN8-type spectrum at the light minima. Analysis of Gran Telescopio Canarias spectra obtained in 2016 led to the conclusion that it is surrounded by an unresolved H II region formed mostly of ejected material from the central star and revealed the presence of a second, more extended asymmetrical emission region.
*Aims.* The aim of this paper is to further explore the structure of the nearby environment of GR 290.
*Methods.* Long-slit spectra of GR 290 were obtained with three slit orientations in the visual and red spectral regions. The emission-line distribution for each slit was analyzed.
*Results.* We confirm the presence of an asymmetric H II region that extends ∼50 pc to the south; ∼30 pc to the north, and southeast; ∼20 pc to the east and northwest; and ∼10 pc to the west. We also present the first spectrum to be acquired of a star belonging to the neighboring OB 88 association, J013501.87+304157.3, which we classify as a B-type supergiant with a possible binary companion.

**Key words.** stars: variables: S Doradus – stars: Wolf-Rayet – stars: evolution – stars: winds, outflows – galaxies: individual: M33 – stars: individual: Romano's star

## 1. Introduction

Evolved massive stars are generally associated with H II regions that may consist of leftover gas from the star formation epoch and a combination of shells and wind ejected by the star during the different stages of its evolution. In general, as soon as a massive star is born, its fast wind interacts with the remaining gas in the vicinity, propelling it outward. At later times, mass is lost in the form of a slow wind or shell ejections during the luminous blue variable (LBV) evolutionary stage (Vink 2012), which is then followed by the Wolf-Rayet (WR) stage (Crowther 2007) in which the more powerful wind mixes into the previously ejected material (see e.g. Lozinskaya 1992). The final interaction occurs when the star ends its life in a supernova explosion and the ejecta violently impact the surrounding interstellar medium (ISM).

Information on the evolutionary path of the central star may be derived from studying the chemical composition and morphology of its surrounding ISM structures (Gvaramadze et al. 2010; Weis 2012; Martayan et al. 2016). Structures with a chemical composition that is enriched with nuclear processed elements suggest that the parent star is in an evolved state. Asymmetries suggest the presence of an inhomogeneous initial ISM, nonspherical mass ejections, or interaction with winds of a binary companion or of nearby sources (Lozinskaya 1992).

Few studies have been performed of H II regions surrounding individual stars in M 33, and fewer still of the ISM environment of LBVs in this galaxy. Therefore, the study of GR 290 (M 33 V0532 or Romano's star), classified as an LBV candidate (Romano 1978; Humphreys & Davidson 1994), but suspected of being a post-LBV star transitioning into the WR phase (Polcaro et al. 2016), is extremely relevant. Its long-term photometric behavior includes a rise to maximum brightness ($B$ ∼16.1 mag) in the 1990s and a slow decline interrupted by brief brightness enhancements (Polcaro et al. 2016). Since 2013, GR 290 is at its historically faintest state with $V = 18.7-18.8$ mag (Calabresi et al. 2014; Maryeva et al. 2019). The photometric variations are accompanied by spectral changes. During the visual maximum of 1992 the star presented a B-supergiant spectrum (Szeifert 1996), while in all subsequent observations its spectrum was

⋆ Based on observations made with the Gran Telescopio Canarias (GTC), installed at the Spanish Observatorio del Roque de los Muchachos of the Instituto de Astrofísica de Canarias, in the island of La Palma and with the Cassini 1.52-m telescope of the Bologna Observatory (Italy).

that of a nitrogen sequence Wolf-Rayet (WN) star (Sholukhova et al. 2011). A history of the study of GR 290 is summarized in the review by Maryeva et al. (2019). Its wind is overabundant in He and N and underabundant in C and O compared to the typical M 33 chemical abundances (Maryeva et al. 2018, hereafter Paper I). Therefore, depending on the age of the system, its nearby environment should reflect the evolving wind conditions.

A recent analysis of long-slit spectra obtained with the Gran Telescopio Canarias (GTC) showed that GR 290 is surrounded by a compact unresolved (0.8–4 pc) nebula with chemical abundances that, with the exception of oxygen, are similar to the current stellar wind abundances (Paper I). Therefore, this nebula originated primarily from stellar ejecta, and one might expect the presence of a larger, wind-blown bubble formed earlier during the O-star evolutionary phase. Indeed, the same study reported a partially resolved H II region extending ∼11 pc to the east and ∼5 pc to the west[1]. This asymmetry is not a priori expected from a wind-blown bubble unless it is expanding into an inhomogeneous medium or asymmetric mass loss occurs. The latter was suspected by Fabrika et al. (2005) who reported the tentative discovery of an ISM structure centered on GR 290 and running northeast–southwest, with a velocity field suggesting a bipolar outflow.

Interaction of the circumstellar material of GR 290 with nearby stellar wind sources might also lead to asymmetries. Although this star is located in a relatively isolated region, it is ∼200 pc to the east of the OB 89 star cluster (Humphreys & Sandage 1980; Ivanov et al. 1993; Massey et al. 1995). This raises the possibility of an interaction between the cluster wind and that of the O-star progenitor of GR 290.

This paper is a continuation of the work we started in Paper I, where a detailed analysis of the stellar spectrum was presented, focusing on the physical properties of the star which is currently in a deep brightness minimum. In addition, the long-slit spectra suggested the presence of an extended nebular region. Here we concentrate solely on the properties of its circumstellar nebula. Therefore, the paper presents an analysis of the spatial extent and asymmetry of nebular emission around GR 290 based on a dedicated set of long-slit spectral observations performed with GTC/OSIRIS with three slit orientations. In Sect. 2 we describe the observations and data-reduction process. Section 3 describes the properties of the extended nebula, which is then discussed in Sect. 4. In Sect. 5 we present the conclusions. In the appendix, we also present the spectrum of hot star J013501.87+304157.3 obtained serendipitously during our observations.

## 2. Observations

GR 290 was observed with the OSIRIS spectrograph on the Gran Telescopio Canarias (GTC) on 2018 September 8, in Service Observing mode. The seeing was stable at the level of 0.8−0.9″. The instrument was configured to use R2500V gratings for the visual (4500–6000 Å) and R2500R for the red (5575–7685 Å) ranges, and a long 7.4′ slit with a width of 0.6″. A summary of the slit position angles (PAs), the exposure times ($t_{exp}$), and the spectral resolution and signal-to-noise ratio (S/N) ranges is presented in Table 1. For future reference, similar observations obtained in 2016 used a slit position of PA = 94.75° and a seeing was 0.9–1.1″.

[1] Here and in what follows we adopt a distance of 847 kpc which leads to a scale of 1.06 pc pixel$^{-1}$ (0.258 arcsec pixel$^{-1}$) for GTC/OSIRIS.

**Table 1.** Spectroscopic observations from 2018 September 8.

| PA (deg) | MJD | Filter ID | $t_{exp}$ (s) | Å/pix | $S/N$ |
|---|---|---|---|---|---|
| 0 | 58 370.03991 | R2500V | 900 | 0.80 | 30–49 |
| | 58 370.05080 | R2500R | 600 | 1.035 | 18–25 |
| 135 | 58 370.07376 | R2500V | 900 | 0.80 | 30–48 |
| | 58 370.08464 | R2500R | 600 | 1.035 | 25–29 |
| 90 | 58 370.10314 | R2500V | 900 | 0.80 | 28–41 |
| | 58 370.11402 | R2500R | 600 | 1.035 | 21–27 |

The spectra were reduced using the ScoRe package[2] initially created for the reduction of data acquired with the SCORPIO spectrograph[3]. ScoRe was used to perform all the standard stages of the long-slit data reduction process: bias and flat field corrections, linearization, flux calibration using a G191-B2B spectroscopic standard star, and an extraction of spectrum along the dispersion using robust Gaussian fitting, analogous to how it was done in Maryeva & Abolmasov (2010). We also removed night sky lines from two-dimensional spectral images by interpolating them using the blank regions outside the studied objects.

The wavelength calibration was performed using the calibration lamp spectra that were acquired on the morning following the GR 290 observations. We find that there is a shift in the lines of the GR 290 spectrum obtained with the PA = 0 slit compared to those in the spectra obtained with the other two slits. To correct for this discrepancy, we used the telluric lines to refine the wavelength calibration.

Contemporaneous photometric observations were obtained on 2018 September 13 (MJD 58374) using the 1.52 m Cassini Telescope run by INAF-Osservatorio Astronomico di Bologna in Loiano. The brightness of GR 290 was: $B = 18.65 \pm 0.04$ mag, $V = 18.73 \pm 0.04$ mag and $R = 18.63 \pm 0.04$ mag, confirming that the GTC observations were obtained during a deep visual minimum of the star.

## 3. Results

The spectra of GR 290 itself in all acquired data sets with different slit orientations are identical within the error bars. Figure 1 shows the result of a co-addition of these three spectra. The object spectral type is WN8h, typical for GR 290 at minimum brightness, and is nearly identical to that obtained in 2016 when the star was at $V = 18.77$ mag (Paper I; Maryeva et al. 2019). In particular, the ratio of equivalent widths (EWs) of He II4686/H$\beta \simeq 0.9$ remains unchanged within error bars, though the EWs of both lines were slightly smaller back in 2016. This equivalent width increase can be traced to an increase by $\sim 33 \pm 7$ km s$^{-1}$ in the line width, although the peak intensity remained constant. Except for that, overall spectral properties are practically identical to the ones described in Paper I, which corresponds to the star being in a stable deep minimum of brightness since 2013 (Maryeva et al. 2019). Therefore, we do not further discuss the spectral properties of the star itself, concentrating solely on the extended nebular component.

[2] SCORE package http://favor2.info/score/score.html

[3] SCORPIO is Spectral Camera with Optical Reducer for Photometric and Interferometric Observations (SCORPIO) on the Russian 6 m telescope.

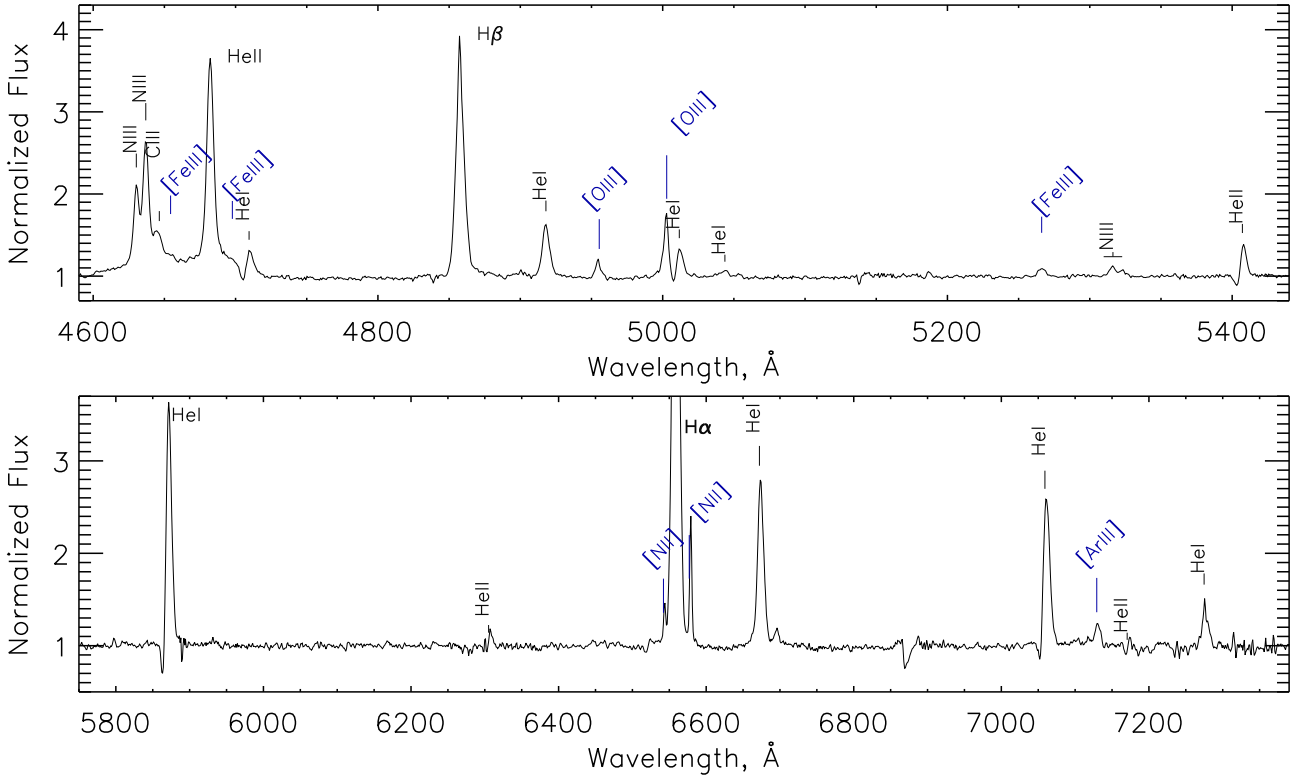


**Fig. 1.** Normalized spectrum of GR 290 obtained on 2018 September 8, derived by co-adding all three acquired spectra with different orientations of the slit. Principal emission lines are identified.

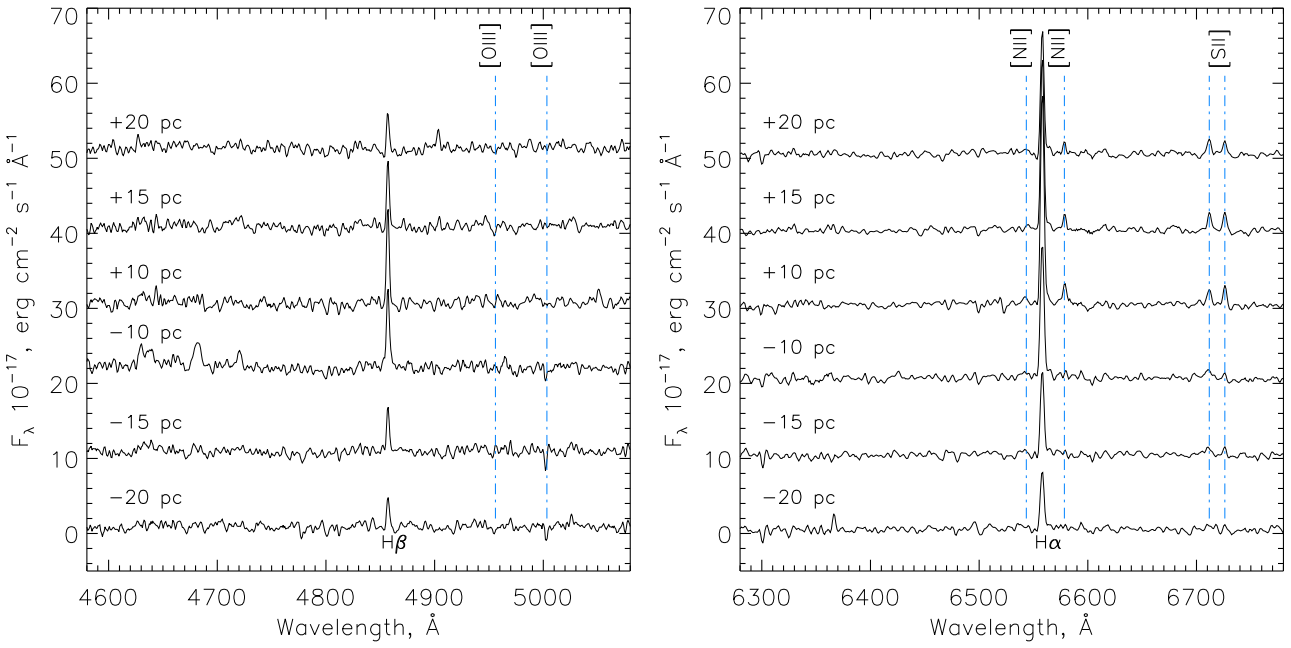


**Fig. 2.** Emission spectra of a nebula in the regions extracted from a two-dimensional spectral image, corresponding to slit PA = 135° (orientated southeast-northwest; see Table 1 and Fig. 3) at different distances from the star. For clarity, the spectra are shifted vertically, and the original baseline of every spectrum is equal to zero. Spectra are extracted in apertures of 5 pixels in width, corresponding to a spatial resolution of 5.3 pc. The spectra are centered on H$\beta$ (*left panel*) and H$\alpha$ (*right panel*); no other spectral region contains any detectable nebular line.

Figure 2 shows sample spectra of the nebula extracted at different distances from the central star for one of the slit orientations. Only H$\alpha$, H$\beta$, [N II], and [S II] lines are detectable there, and no other line shows any spatially extended component. For example, the nebular oxygen doublet [O III] 4959, 5007 Å is clearly visible in the spectrum of the star itself (see Fig. 1) but is not detectable in the extended nebula, which is consistent with it being formed only in close proximity to the star

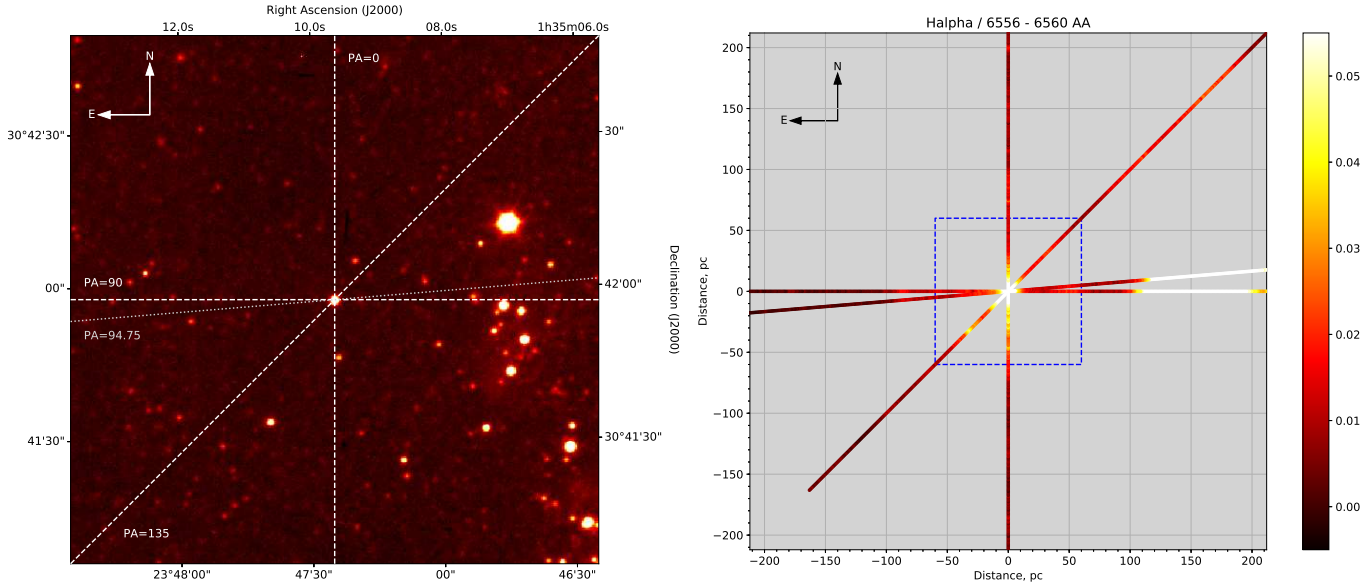


**Fig. 3.** *Left*: identification chart for a 100″ wide region around GR 290 in the Sloan $g$ filter image illustrating the slit positions used during the 2018 observations (dashed lines), as well as during the 2016 (dotted line). The axes are given in RA and Dec and the position angle of each slit is listed. The stellar association OB 89 is located to the right (West) of GR 290. *Right*: spatial distribution of the H$\alpha$ intensity along each of the three slits. The orientation and scale of the image is the same as in left panel, but here the axes are given in linear distance (pc) from GR 290, which lies at the center of the coordinate system. Distance is computed assuming a 1.06 pc pix$^{-1}$ scale along the slit. The strongest emission is color coded in white. Extended emission is evident south and east of GR 290. The dotted square defines the ±60 pc subregion that we analyze in detail.

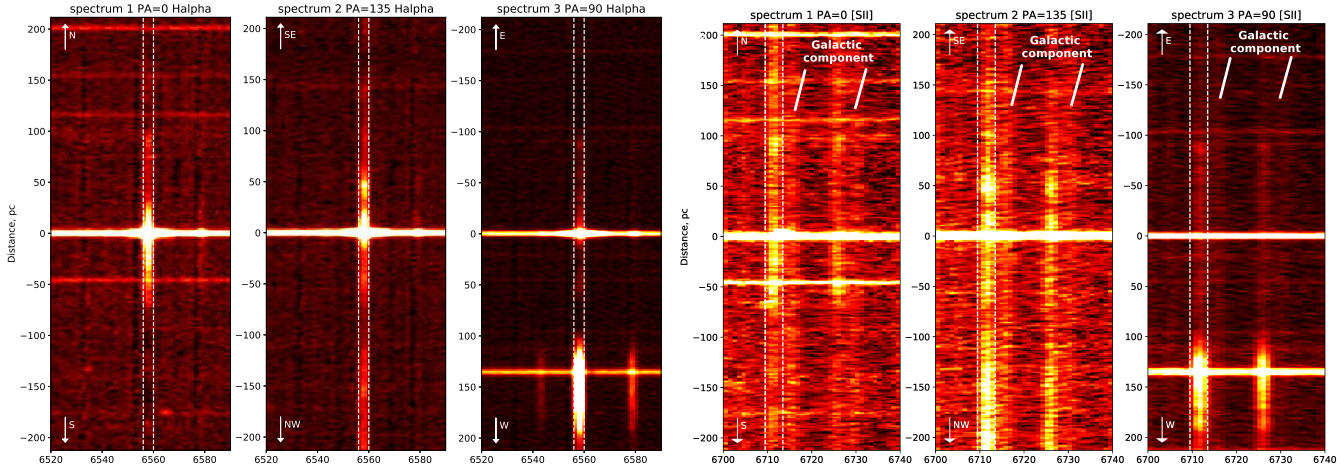


**Fig. 4.** Spatial distribution (vertical axis, given in pc) of the emission along the slit in the wavelength intervals (horizontal axis) 6520–6590 Å (*left panels*) and 6700–6740 Å (*right panels*), for three slit orientations. The vertical dimension is the same as that of the dimensions in the identification chart shown in Fig. 3. Arrows at the top and bottom of each image indicate the orientation. The aperture size that was used for the extraction of H$\alpha$ and [S II] along each slit is indicated with the white dashed lines. *Right panels*: the Galactic [S II] emission is also visible to the right of the M 33 emission. Dark faint traces along the vertical axis are residual marks of subtraction of night sky lines from the images, done mostly for cosmetic and presentational purposes.

(in Paper I we estimated the size of this inner nebula to be 0.8–4 pc). On the other hand, the spectrum of the star lacks sulphur lines [S II] 6717, 6731 Å apparent in the extended emission; we specifically discuss these lines below. The intensity ratio of H$\alpha$ to H$\beta$ remains constant with distance from the star and close to 3 (Brocklehurst 1971), which corresponds to an extended H II region with negligible reddening (indistinguishable from Galaxy foreground extinction $E_{(B-V)} = 0.052$ towards M33 according to the NASA/IPAC Extragalactic Database (NED) extinction calculator, Schlegel et al. 1998).

The two-dimensional spectral images obtained with GTC provide information on the diffuse emitting regions in the neighborhood of GR 290. The slit orientations were selected to probe the ISM content along six rays extending outward from GR 290, both coincident and perpendicular to the one used in observations of 2016 (Paper I), as well as spanning in one more direction to have better constraints on the nebular shape. Slit positions in the immediate 100″ neighborhood of the object are shown in Fig. 3 (left) superimposed on the direct image of the region, acquired also with GTC in the Sloan $g$ filter. For each orientation, we extracted the emission along the slit at the positions of H$\alpha$, H$\beta$, He I, [N II], [O III], and [S II] lines using background-subtracted flux summation inside apertures of 4–5 pixels (which roughly corresponds to 4–5 Å) wide, as illustrated in Fig. 4.

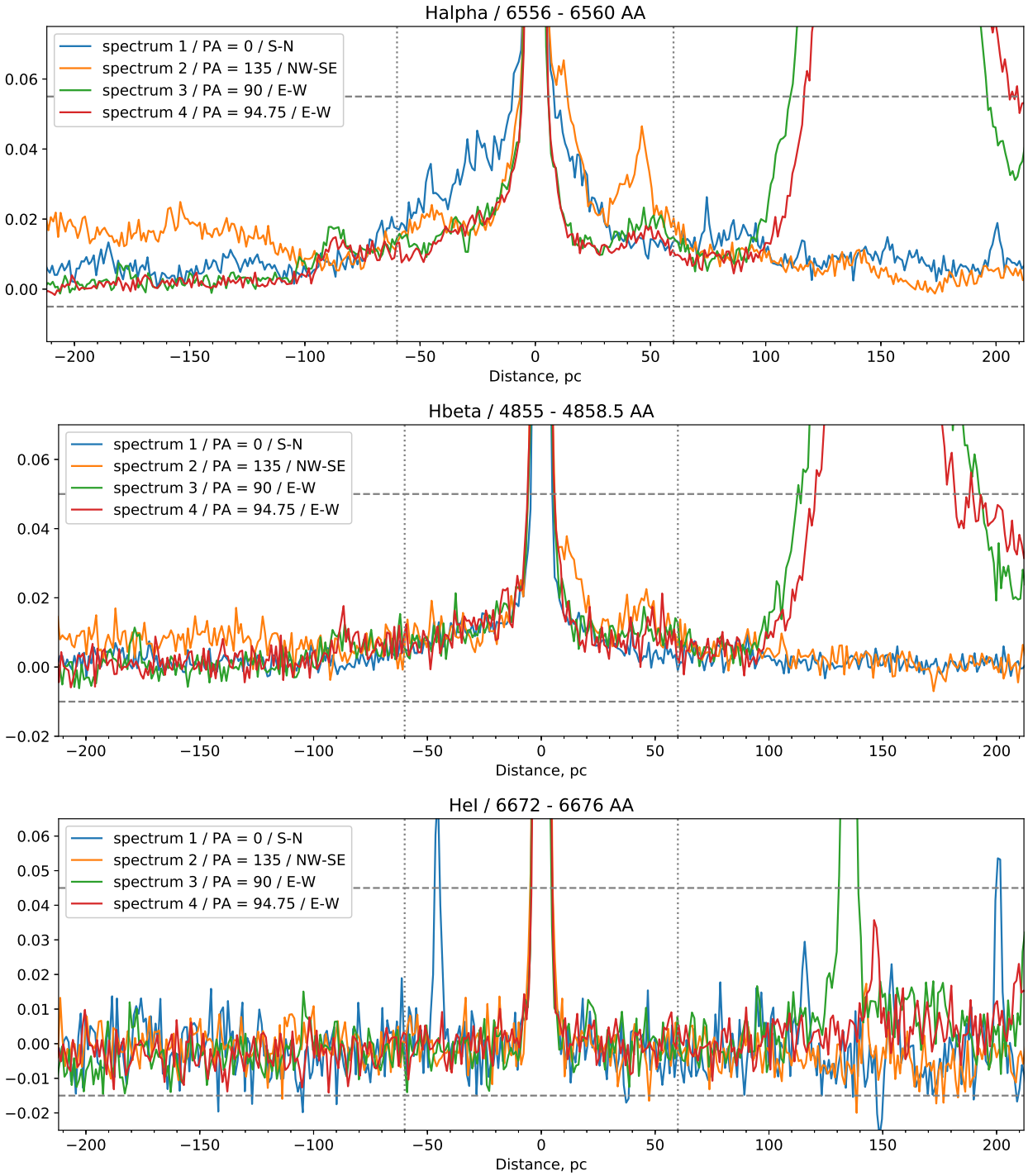


**Fig. 5.** Tracings of the intensity of H$\alpha$, H$\beta$, and He I along the slit allowing a comparison of the spatial distribution of these emissions in the vicinity of GR 290. The horizontal axis is the linear distance from GR 290 in parsecs. The vertical axis gives the scaled intensity, with a scaling such that the maximum intensity of each line is set to unity. The horizontal lines indicate the intensity interval (6% of a peak intensity) used to define the black-to-white scale shown in Figs. 3 (right) and 7. The vertical lines enclose the ±60 pc subregion shown in Fig. 7. Each panel is labeled with the wavelength interval on the observed spectrum before correcting for the M 33 radial velocity. The same tracings for [N II] and [S II] are shown below in Fig. 6.

The extraction apertures were defined so as to include the totality of the extended emission, with their widths and positions corresponding to the [−310:−130] km s$^{-1}$ range of velocities, consistent with the −179 km s$^{-1}$ heliocentric velocity of the M 33 galaxy. Where visible, the extended emission in these lines has a simple one-peak structure with no signs of a velocity gradient within the data precision of about 50 km s$^{-1}$.

The profile of H$\alpha$ emission, scaled to the maximum intensity value and color coded, is presented in Fig. 3 (right), where the coordinate axes show the distance from GR 290, computed adopting a 1.06 pc pix$^{-1}$ scale along the slit. Its asymmetry is evident there, as the PA = 0° slit shows that emission is more extended towards the south than to the north. Similarly, the emission in the PA = 135° slit is more extended towards the

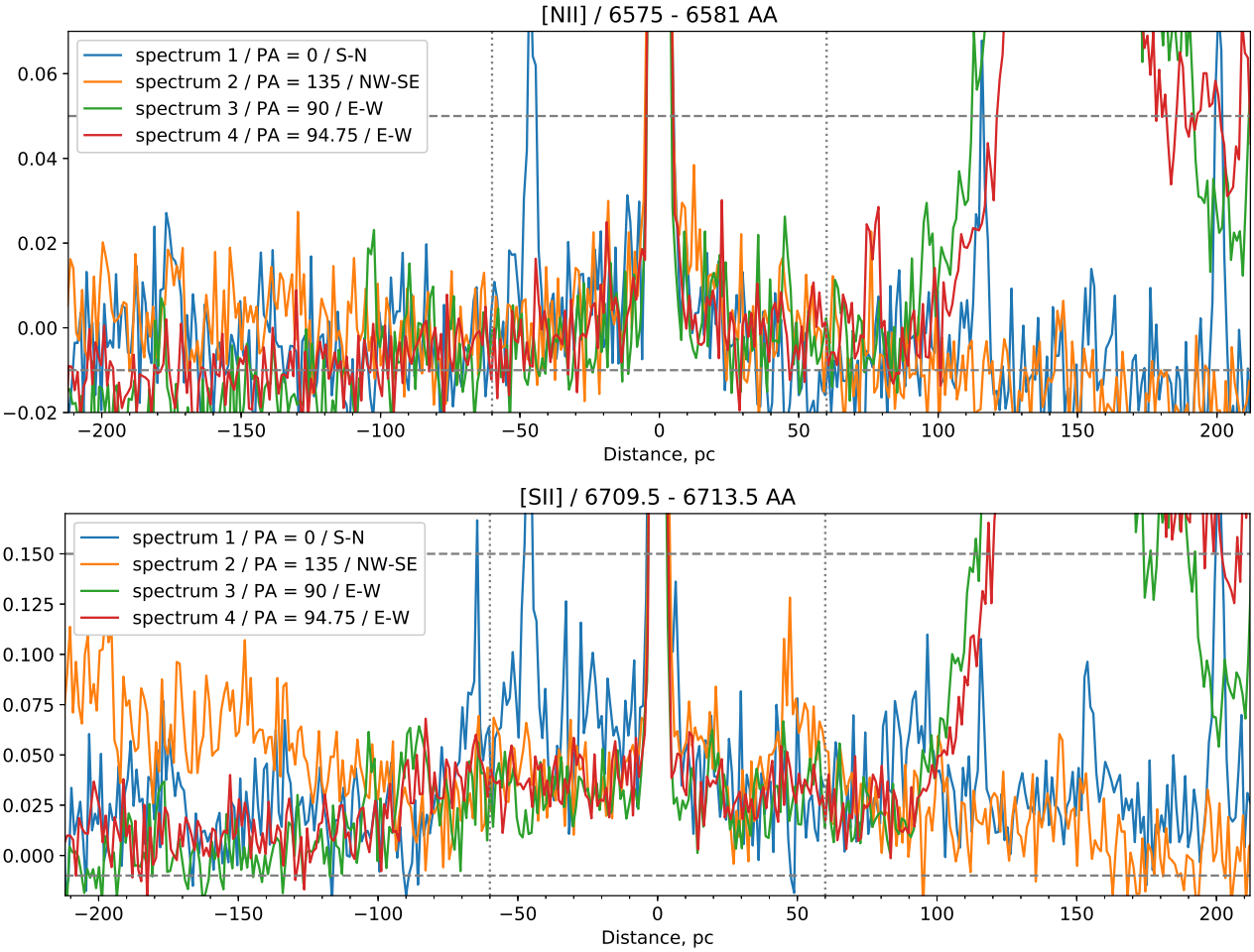


**Fig. 6.** As in Fig. 5 but for [N II] and [S II].

southeast and that of the PA = 90° slit is more extended towards the east. Evidence of an asymmetric nebula visible in Balmer lines was previously reported in Paper I based on observations obtained with a slit having an approximately east–west orientation (PA = 94.75°, also shown in Fig. 3). All these data show that the strongest asymmetry actually appears in the SE–NW direction (slit PA = 135°).

In order to better evaluate the dimensions of the circumstellar structures, we present in Fig. 5 (top) the tracings of the scaled H$\alpha$ emission intensity along the spatial coordinate. Here we see that the resolved nebula surrounding GR 290 extends ∼50 pc south; ∼30 pc north and southeast; ∼20 pc east and northwest; and ∼10 pc west. Noteworthy is the appearance of two peaks in the SE orientation: one at ∼15 pc and the second at ∼45 pc. The latter two structures are clearly visible also in the H$\beta$ tracings shown in the second panel of Fig. 5, confirming their existence. The more distant of these emission peaks shows up in the second panel of Fig. 4 as a separate source, although there is no stellar counterpart visible in the direct image (see Fig. 3). This region is clearly extended.

The bottom panel of Fig. 5 shows the tracing of He I 6678. This line is formed mainly in the stellar atmosphere. Its spatial profile, extending over <5 pc in each direction, is nearly identical in the three slit positions, and reflects the spatial resolution of our data. The [O III] lines do not show an extended structure, while the low S/N prevents a clear assessment of the complex structure of [N II] lines (Fig. 6).

The E–W slit crosses the northern portion of the OB 89 association, and the corresponding tracings in Fig. 5 show that the emission arising in the association extends for approximately 100 pc, its edge being located just ∼100 pc from GR 290.

The behavior of sulphur lines is significantly different from that of the hydrogen lines. [S II] 6717, 6731 Å lines are absent in the spectrum of GR 290 (see Fig. 1) and we do not consider it as coming from the nebula itself. The right panel of Fig. 4 shows that both of these lines have two components. The line-of-sight velocity of the blueshifted component corresponds to the systemic velocity of the M 33[4], while the redshifted component has a velocity of about 0 km s$^{-1}$. The latter component has a uniform distribution of the flux along the slit. We hypothesize that only the blueshifted component is related to the emission from M 33, while the second component probably corresponds to foreground emission of the diffuse ionized gas (DIG) in our Galaxy which is characterized by enhanced [S II] emission (see e.g., Haffner et al. 2009). The emission from DIG of the Galaxy might contaminate the spectra of extragalactic objects in the case of their relative proximity to the Galactic plane (e.g. it was clearly shown by Efremov et al. 2011 for the NGC 6946 galaxy). In the further analysis, we use only the blueshifted component of [S II], corresponding to the gas in M 33. This component is strongly inhomogeneous and is observed in the nebula and also

[4] Systematic velocities of M 33 is −179 km s$^{-1}$ (Lavaux & Hudson 2011) and a heliocentric correction is +20 km s$^{-1}$.

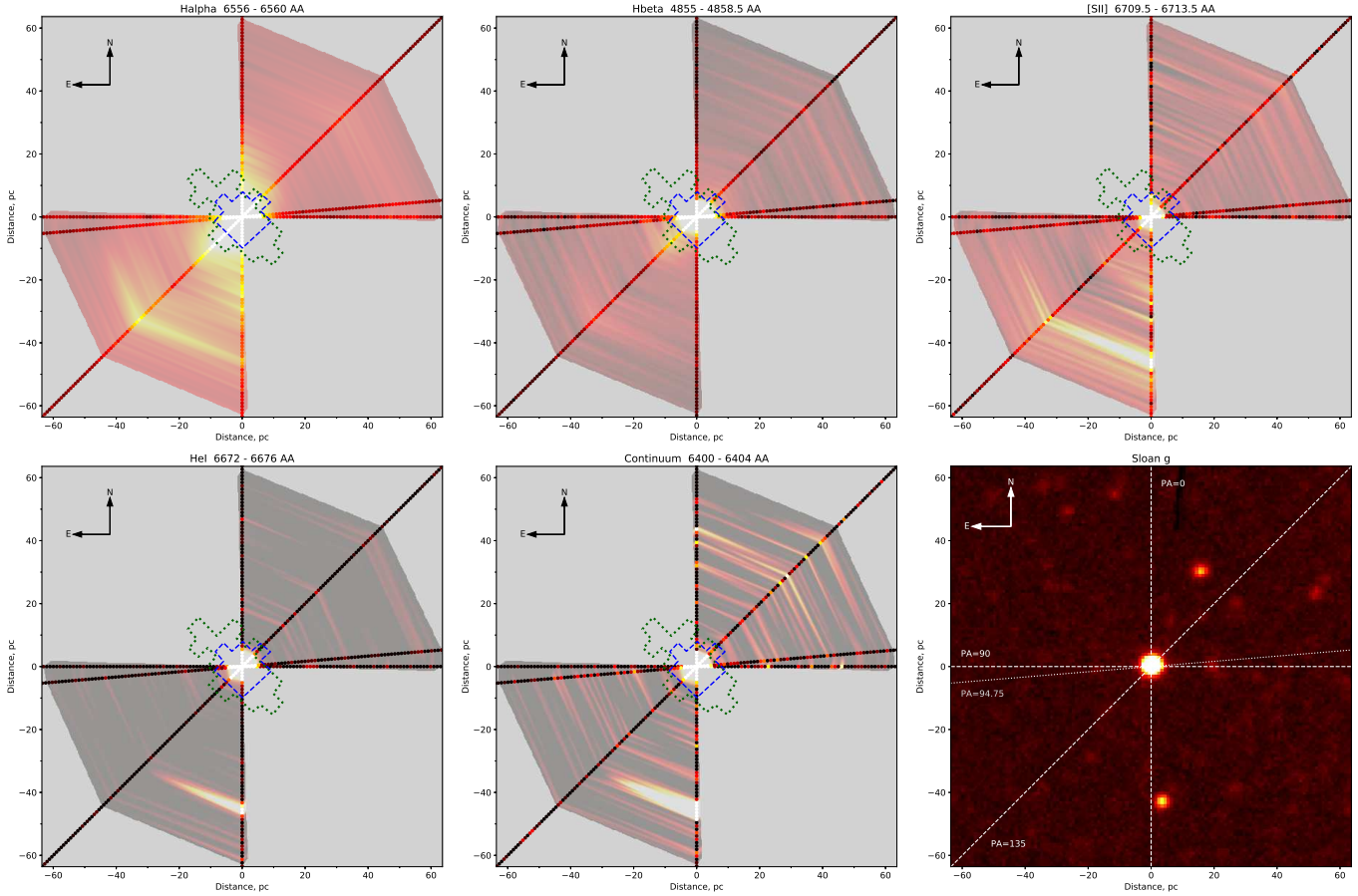


**Fig. 7.** Spatial structure of the H$\alpha$ (*top left*), H$\beta$ (*top middle*), [S II] (*top right*), He I (*bottom left*) and a continuum at 6400 Å (*bottom middle*) emission in the $\pm 60 \times 60$ pc region centered on GR 290 according to the spatial tracings in four slit orientations. Every dot corresponds to a one-pixel (1.06 pc) step along the slit, with black-to-white scale defined as in Figs. 5 and 6 as 6% of a peak line intensity (16% for [S II]). For visual clarity, the rough linear interpolation between these points is also shown in a semi-transparent overlay inside NW–SE sectors where our coverage is dense enough. While it does not necessarily reflect the "true" intensity distribution between the slits and especially in the NE–SW direction where we lack data, it still perfectly depicts the significant asymmetry of the nebula along the NW–SE direction. Blue dashed and green dotted lines mark the extent of the nebula reported by Fabrika et al. (2005) in narrow H$\beta$ intensity and velocity gradient, respectively. Also, for ease of comparison, direct image of the region in Sloan *g* filter with the same scale and orientation is shown in *bottom right panel*, which is a subset of Fig. 3.

at different positions in its vicinity. Variations of its flux are significant, but in general, the trend with the distance from the star is absent. The [S II]/H$\alpha$ ratio drops towards the star which is typical for H II regions, but is primarily due to the increase of H$\alpha$ intensity there. At distances greater than 30 pc the [S II]/H$\alpha$ ratio is about 0.4–0.6, which is a typical value for DIG. We therefore consider these [S II] lines to be mostly a background contribution, probably originating from the DIG in M 33, and therefore unsuitable for additional nebular analysis.

## 4. Discussion

GR 290 is believed to be an object that has already passed through an LBV phase and is becoming a WR star (Polcaro et al. 2011, 2016). It is surrounded by a compact, unresolved nebula with a probable dimension of $R \sim 0.8$ pc and a chemical composition similar to that of the wind of the parent star, suggesting that it consists of material that was ejected during the LBV phase (Paper I).

Our new spectra show the presence of nebular emission regions extending as far as 30 pc south, east, and southeast of the star, but only 10 pc to the west. To facilitate the visualization of the spatial structure of the nebular gas, Fig. 7 shows the "line maps" constructed using a 2D linear interpolation between the intensity points on the lines corresponding to slit positions. These maps cover the ±60 pc region centered on GR 290 shown in the bottom right panel of Fig. 7. The maps use the intensity scale (black-to-white corresponding to 6% of a peak intensity of the corresponding line) marked with a dashed horizontal line in Fig. 5.

We note in Figs. 5 and 6 the presence of a sharp peak in both the He I and [N II] spatial distributions located ~50 pc south of GR 290. This approximately coincides with the projected distance of a stellar object that is visible in the bottom right panel of Fig. 7 slightly to the west of the slit position. Thus, part of the southern extension seen in H$\alpha$ and H$\beta$ could be attributed to gas that is associated with this object. As the spectrum of GR 290 lacks [S II], we may conclude that its spatial structure reflects the distribution of a warm interstellar gas. Therefore, the weak spot in H$\alpha$ at about 20 pc to the south of GR 290 is probably also related to this warm interstellar gas. On the other hand, there is nothing else visible within 60 pc towards the east and southeast of GR 290, and therefore we may conclude that the spatial structure of the 50 pc emission does indeed form part of an H II region that is associated with GR 290. The size of the nebula around GR 290 detected by us is close to the one around another LBV

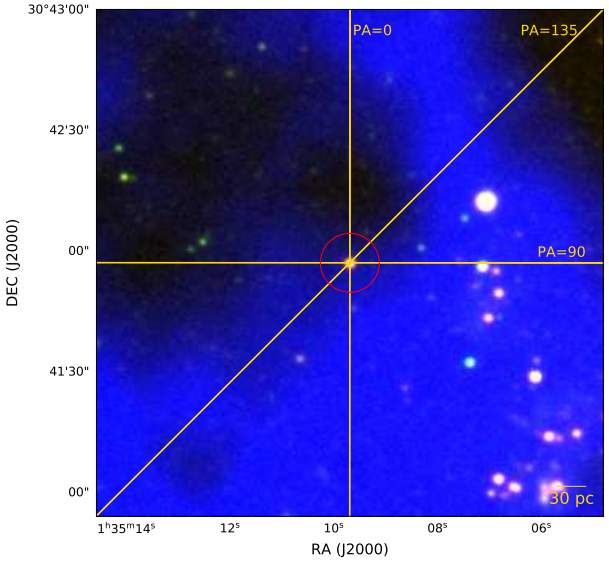


**Fig. 8.** Distribution of the neutral gas in the vicinity of GR 290. The color picture is a combination of three direct images, with the blue channel corresponding to H I 21 cm from Gratier et al. (2010), green to that from SDSS-g and red to that from SDSS-r. The position of GR 290 is marked by a red circle with a radius corresponding to 30 pc.

star in M 33, Var 2, which is most likely a result of O-star winds (Burggraf et al. 2005). According to the estimation by Burggraf et al. (2005), the diameter of the nebula around Var 2 is 54 pc. Thus, based on the similarity of size and evolutionary status of GR 290 we may tentatively conclude that the extended nebula around GR 290 also resulted from mass loss during the O-star phase.

GR 290 lies in an outer arm of M 33 at a distance ∼17′ from the galaxy center. In the same arm and at a similar distance (∼15.5′ from the center, and ∼4′ from GR 290) there are two O9 stars with unusually large (diameters of ∼130 pc) and perfectly spherical H II regions – CPSDP 362 and CPSDP 364 (Oey & Massey 1994; Courtes et al. 1987). Such a difference in the size and shape of the extended H II regions may be due to different ISM environments – influences from a nearby OB 89 association for GR 290, and the much more sparse neighborhoods surrounding CPSDP 362 and CPSDP 364. Indeed, GR 290 lies at a projected E–W distance of ∼200 pc to the east of the OB 89 star association and, as can be seen in Fig. 5, is only ∼100 pc from the edge of the photoionized H II region surrounding it. Thus, the possibility exists that there is additional ISM material beyond the photoionized gas of the association that has inhibited the expansion of the original GR 290 wind-blown bubble in the direction of the cluster.

While most of the known nebulae around WR stars appear to be symmetrical, there are objects in our Galaxy that clearly display a strongly asymmetrical shape (see, e.g., Barlow et al. 1976 and Dopita & Lozinskaia 1990). Usually, the asymmetrical shape of the nebula is explained as a result of the inhomogeneities in the surrounding ISM. That is, strong stellar wind and ejecta from WR stars blow out asymmetrical bubbles in the presence of density gradients in the surrounding ISM that are asymmetrical. In order to check our hypothesis regarding the density gradients in the surrounding ISM we searched for archival data on the neutral gas distribution in this part of the M 33 galaxy. Figure 8 demonstrates the relative distribution of the H I 21 cm column density in the vicinity of GR 290 from Gratier et al. (2010). It is clearly seen that while the nearby OB associations are located in the extended dense cloud of H I, the GR 290 is observed toward the edge of the local shell in the H I distribution. While the influence of the wind from GR 290 during the WR and previous stages might contribute significantly to the evolution of this shell, its size is much larger than expected for bubbles created by single WR stars. Hence, we may conclude that this H I shell was created independently from the influence of GR 290, and because the LBV is observed toward the edge of this shell, it is very probable that its wind acts in the inhomogeneous surrounding medium.

Fabrika et al. (2005) marginally resolved the circumstellar nebula of GR 290 using integral field spectroscopic observations in H$\beta$. These latter authors found a slight excess in the narrow (with ∼4Å $FWHM$) line component extending for up to 5″(∼20.5 pc) from the object, and a velocity gradient across the region extending for about ∼30 pc from the southwest towards northeast: −219 km s$^{-1}$ in the central part (mainly the stellar velocity),−191 km s$^{-1}$ in the southwest, and −235 km s$^{-1}$ in the northeast. Therefore, part of this nebula is approaching the observer and part is receding, as in the case of a bipolar outflow inclined with respect to the sky plane.

Due to the layout of the slits used in our observations (see Fig. 3) we cannot confirm the extent of the nebula in the SW–NE direction, and in other directions the extent in our data is clearly detectable up to 50 pc (SE direction) from the object. On the other hand, the brightest part of H$\alpha$ and H$\beta$ extended emission components are indeed confined within ∼20 pc (see Fig. 5), and therefore the difference in nebular size may be due to the improved sensitivity of our observations. Nondetection of any velocity gradient in our data is also consistent with the primary direction of velocity gradient in the data of Fabrika et al. (2005).

## 5. Conclusions

We present the results of new observations of the WR/LBV object GR 290 (Romano's star) obtained with GTC in September 2018. During the observations we obtained spectra with three different PAs (0°, 90°, and 135°). Combining the results of the new analysis of 2D spectra and the results of calculations using the CLOUDY photoionization code from Paper I we come to the following conclusions:

- GR 290 is surrounded by an elongated small H II region which may have been formed in a previous evolutionary phase of the central star. This region extends ∼50 pc to the south; ∼30 pc to the north and southeast; ∼20 pc to the east and northwest; and ∼10 pc to the west.
- Nebular forbidden lines [N II] and [O III] form in an unresolved region near the star. These observations also confirm the size estimates based on CLOUDY calculations (Paper I), according to which the radius of the circumstellar regions does not exceed 4 pc, with the preferred diameter being 2 pc.

New observations presented here confirm and extend the discovery of an asymmetrical nebula around GR 290 presented in Paper I, consistent with a tentative detection by Fabrika et al. (2005). While they are not sufficient to reveal the entire morphology of this nebula, these observations definitely indicate that the diffuse emission is asymmetrically distributed towards the south and southeast. These results form a reliable basis for future observations, for instance with an integral field spectrograph, in order to establish further details of the asymmetric morphology.

*Acknowledgements.* We thank the GTC observatory staff for obtaining the spectra and Antonio Cabrera-Lavers for guidance in processing the observations. Partial support for this investigation, including the travel grant for O.M.

to visit Mexico, was provided by UNAM/DGAPA/PAPIIT grant IN103619, which is gratefully acknowledged. The work is also partially funded from the European Union's Framework Programme for Research and Innovation Horizon 2020 (2014-2020) under the Marie Skłodowska-Curie Grant Agreement No. 823734. O.M. acknowledges support from the Czech Science Foundation GA18-05665S and Russian Foundation for Basic Research (RFBR) grant 19-02-00779. The Astronomical Institute Ondřejov is supported by the project RVO:67985815. G.K. acknowledges support from CONACYT grant 252499. S.K. acknowledges for support European Structural and Investment Fund and the Czech Ministry of Education, Youth and Sports (Project CoGraDS – CZ.02.1.01/0.0/0.0/15_003/0000437) as well as Russian Government Program of Competitive Growth of the Kazan Federal University. T.L. and O.E. acknowledge support from the RFBR grant 18-02-00976 and from the Program of development of M.V. Lomonosov Moscow State University (Leading Scientific School "Physics of stars, relativistic objects and galaxies"). O.E. acknowledges the Foundation of development of theoretical physics and mathematics "Basis".

## References

Barlow, M. J., Cohen, M., & Gull, T. R. 1976, MNRAS, 176, 359
Brocklehurst, M. 1971, MNRAS, 153, 471
Burggraf, B., Weis, K., & Bomans, D. J. 2005, AIP Conf. Ser., 783, 33
Calabresi, M., Rossi, C., Gualandi, R., et al. 2014, ATel, 5846, 1
Courtes, G., Petit, H., Sivan, J. P., Dodonov, S., & Petit, M. 1987, A&A, 174, 28
Crowther, P. A. 2007, ARA&A, 45, 177
Dopita, M. A., & Lozinskaia, T. A. 1990, ApJ, 359, 419
Efremov, Y. N., Afanasiev, V. L., & Egorov, O. V. 2011, Astrophys. Bull., 66, 304
Fabrika, S., Sholukhova, O., Becker, T., et al. 2005, A&A, 437, 217
Gratier, P., Braine, J., Rodriguez-Fernandez, N. J., et al. 2010, A&A, 522, A3
Gvaramadze, V. V., Kniazev, A. Y., & Fabrika, S. 2010, MNRAS, 405, 1047
Haffner, L. M., Dettmar, R. J., Beckman, J. E., et al. 2009, Rev. Mod. Phys., 81, 969
Humphreys, R. M., & Davidson, K. 1994, PASP, 106, 1025
Humphreys, R. M., & Sandage, A. 1980, ApJS, 44, 319
Ivanov, G. R., Freedman, W. L., & Madore, B. F. 1993, ApJS, 89, 85
Lavaux, G., & Hudson, M. J. 2011, MNRAS, 416, 2840
Le Borgne, J. F., Bruzual, G., Pelló, R., et al. 2003, A&A, 402, 433
Lozinskaya, T. A. 1992, Supernovae and Stellar Wind in the Interstellar Medium (New York: AIP Press)
Martayan, C., Lobel, A., Baade, D., et al. 2016, A&A, 587, A115
Maryeva, O., & Abolmasov, P. 2010, Rev. Mex. Astron. Astrofis., 46, 279
Maryeva, O. V., Chentsov, E. L., Goranskij, V. P., et al. 2016, MNRAS, 458, 491
Maryeva, O., Koenigsberger, G., Egorov, O., et al. 2018, A&A, 617, A51
Maryeva, O., Viotti, R. F., Koenigsberger, G., et al. 2019, Galaxies, 7, 79
Massey, P., Armandroff, T. E., Pyke, R., Patel, K., & Wilson, C. D. 1995, AJ, 110, 2715
Massey, P., Olsen, K. A. G., Hodge, P. W., et al. 2006, AJ, 131, 2478
Oey, M. S., & Massey, P. 1994, ApJ, 425, 635
Polcaro, V. F., Rossi, C., Viotti, R. F., et al. 2011, AJ, 141, 18
Polcaro, V. F., Maryeva, O., Nesci, R., et al. 2016, AJ, 151, 149
Romano, G. 1978, A&A, 67, 291
Schlegel, D. J., Finkbeiner, D. P., & Davis, M. 1998, ApJ, 500, 525
Sholukhova, O. N., Fabrika, S. N., Zharova, A. V., Valeev, A. F., & Goranskij, V. P. 2011, Astrophys. Bull., 66, 123
Szeifert, T. 1996, Liege International Astrophysical Colloquia, 33, 459
Vink, J. S. 2012, Eta Carinae and the Supernova Impostors, eds. K. Davidson & R. M. Humphreys, Astrophys. Space Sci. Lib., 384, 221
Weis, K. 2012, ASP Conf. Ser., 465, 213

## Appendix A: J013501.87+304157.3 star

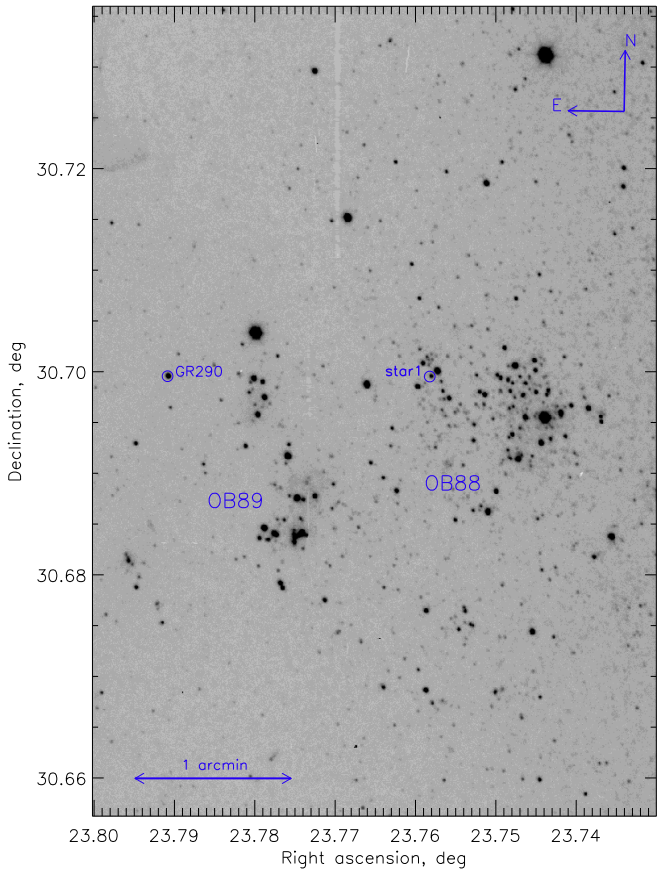


**Fig. A.1.** Identification chart of the star J013501.87+304157.3 marked as "star 1". The image was acquired with GTC in the Sloan $g$ filter.

The long slit used in our observations crossed a number of other stars in the vicinity of GR 290. For five of these, the spectral quality was good enough ($S/N > 10$) to allow the spectra to be extracted. All extracted spectra along with other spectra of stars in the vicinity of GR 290 were published in Maryeva et al. (2019). Here we would like to highlight one of these objects – J013501.87+304157.3 – which attracted our attention by its radial velocity, and to show its spectrum.

This star is located in the OB 88 association and has previously been studied photometrically by Massey et al. (2006). Its identification chart is shown in Fig. A.1. The object displays a hot early-type spectrum, as is shown in Fig. A.2. To perform the spectral classification we used an automatic code based on the $\chi^2$ fitting with spectral standards from STELIB5 (Le Borgne et al. 2003) in the same way as used by Maryeva et al. (2016). According to this code, the preliminary classification of this star is B5 I. For comparison, Fig. A.2 also shows the spectrum of a HD 164353 standard star, which is a typical example of a B5 supergiant.

H$\alpha$ and H$\beta$ absorptions at a velocity of $-50$ km s$^{-1}$ relative to M 33 rest-frame one[5] are prominent in the spectrum, along with signs of a second component in both lines at a velocity of about $+300$ km s$^{-1}$, suggesting the possible presence of a binary companion. We also tentatively identify He I 5015, 5875, and 7065 and C II 6578 and 6582 Å at $-7$ km s$^{-1}$, but these are significantly weaker.

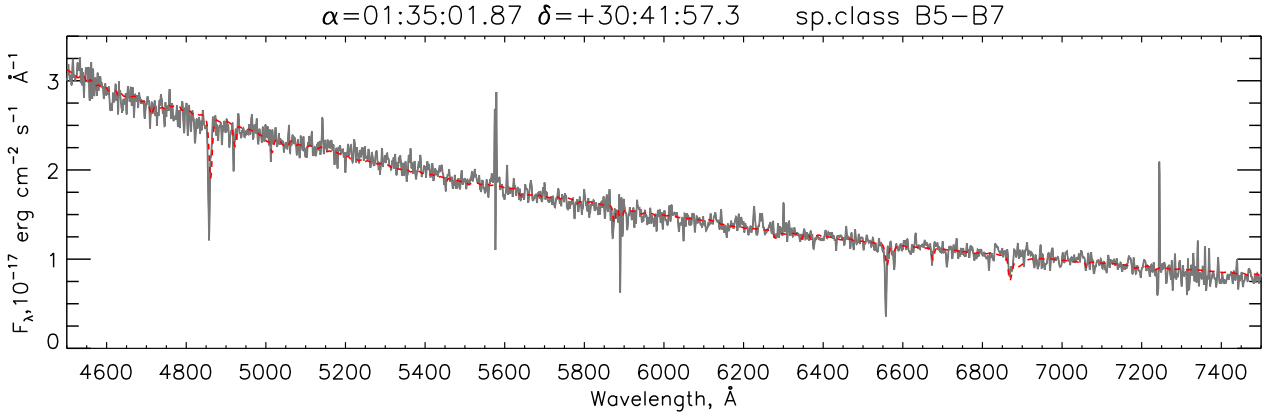


**Fig. A.2.** Spectrum of J013501.87+304157.3. For comparison the reddened spectra of HD 164353 (standard star, typical example of B5 Ib spectral type) is shown by red dashed line.

[5] Velocities are corrected for the adopted M 33 systemic velocity of $-179$ km s$^{-1}$ and a heliocentric correction of $+20$ km s$^{-1}$.